

Supporting Information for

The Reactivity of Nb_n^+ Clusters with Acetylene and Ethylene to Produce a Cubic Aromatic Metal Carbide Nb_4C_4^+

Wen Gan,^{a,b} Benben Huang,^{a,b} Mengzhou Yang,^{a,b} Lijun Geng,^a Zhixun Luo^{a,b,*} and Klavs Hansen^c

^a Beijing National Laboratory for Molecular Sciences (BNLMS), State Key Laboratory for Structural Chemistry of Unstable and Stable Species, Institute of Chemistry, Chinese Academy of Sciences, Beijing 100190, P.R. China.

^b University of Chinese Academy of Sciences, Beijing 100049, P. R. China.

^c Centre for Joint Quantum Studies and Department of Physics, School of Science, Tianjin University, 92 Weijin Road, Tianjin 300072, China.

CONTENTS

S1 Mass Spectrometry Observation.....	2
S2 Optimized Structures.....	4
S3 Energetics	12
S4 Bonding Nature of Nb_4C_4^+	13
S5 Interaction and Energy Decomposition Analysis.....	17
S6 Reaction Dynamics of $\text{Nb}_n^+ + \text{C}_2\text{H}_2$	25

S1 Mass Spectrometry Observation

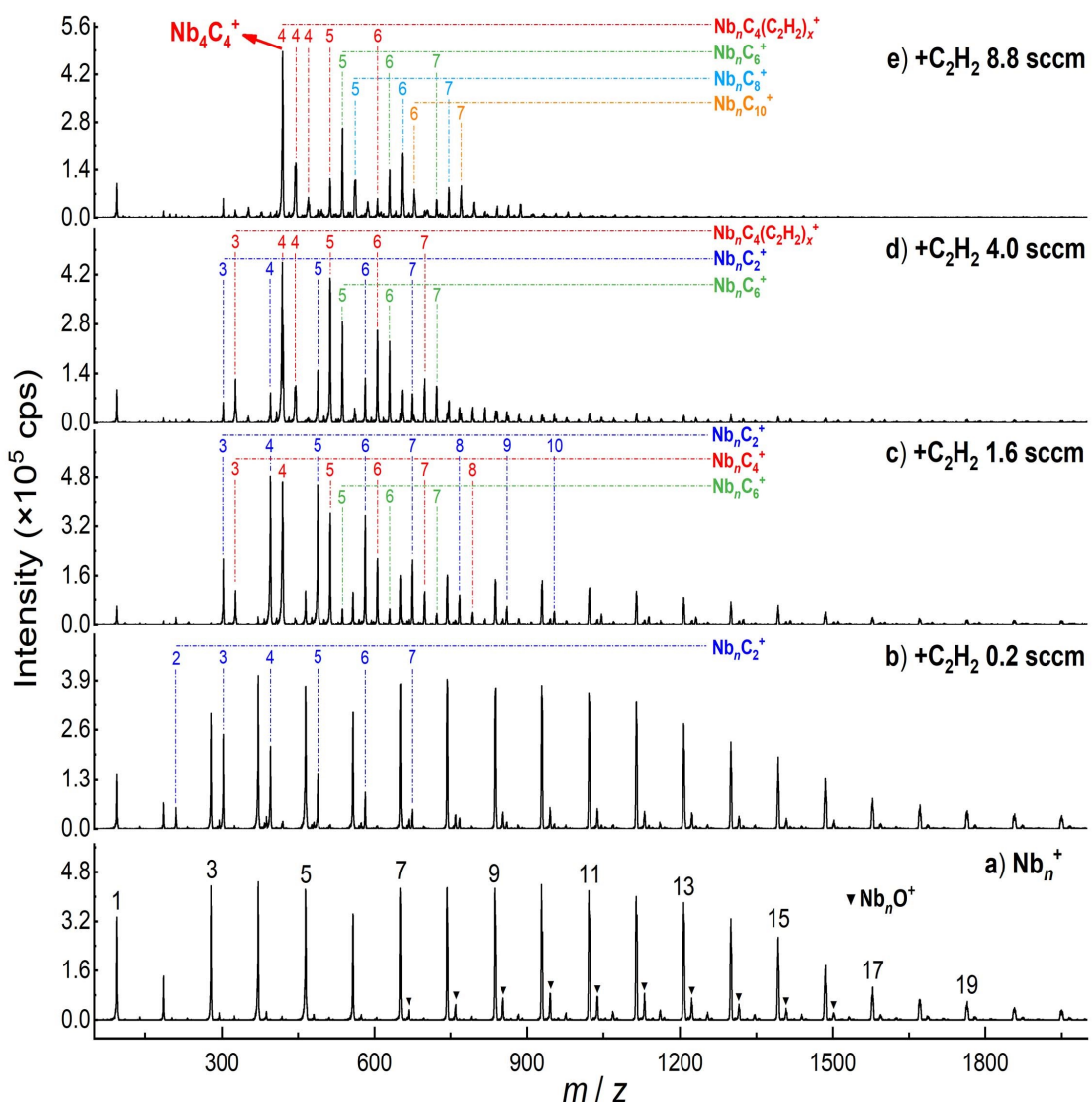


Fig. S1 Repeated experiments showing mass spectra of the Nb_n^+ clusters (a) and reacting with different gas flow rates of 0.2, 1.6, 4.0, and 8.8 sccm 0.2% C_2H_2 in He, respectively (b-e). Those marked with inverted triangle symbols in the bottom frame correspond to oxide contamination.

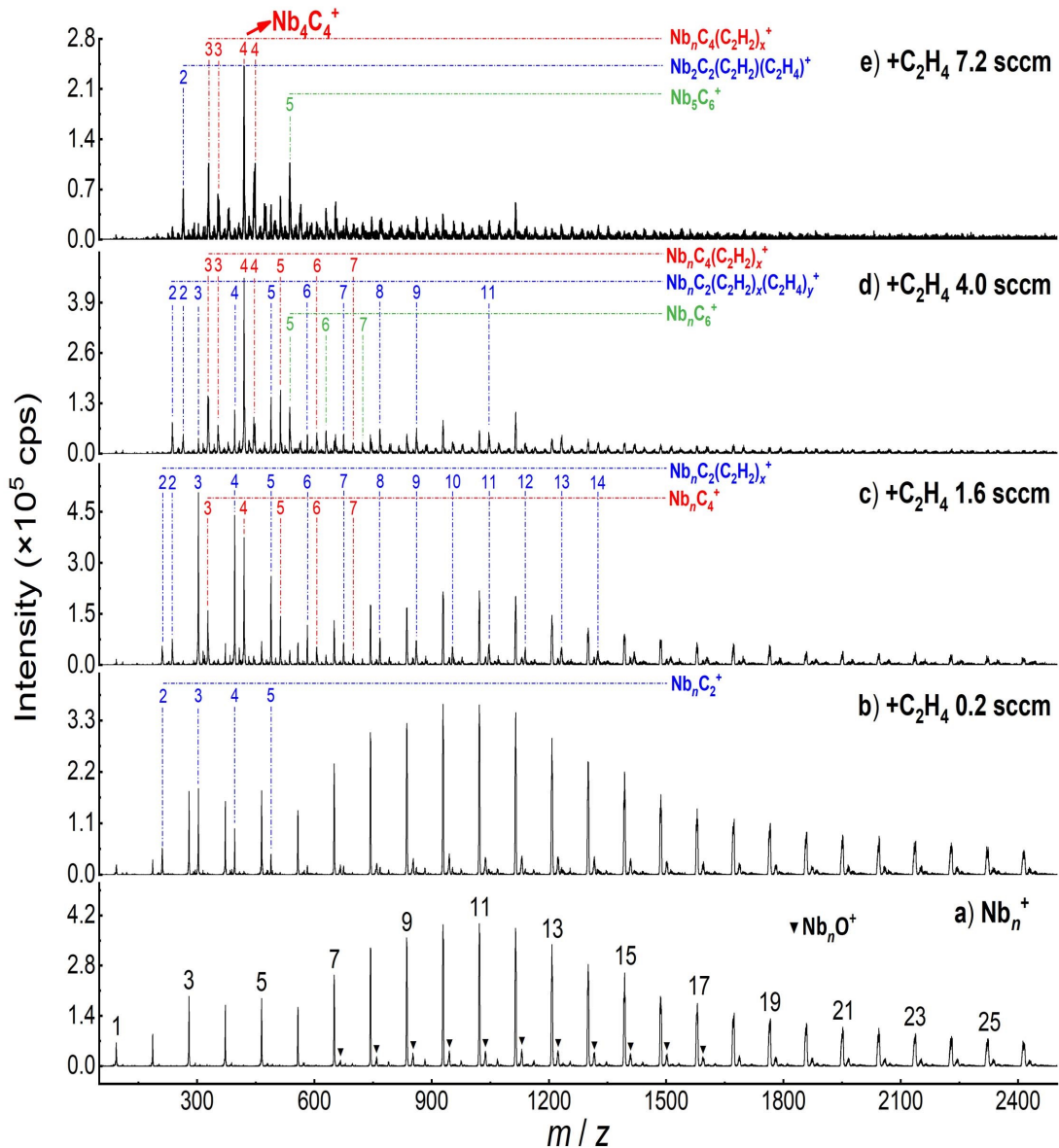


Fig. S2 Mass spectra of the Nb_n^+ clusters (a) and reacting with different gas flow rates of 0.2, 1.6, 4.0, and 7.2 sccm 0.2% C_2H_4 in He, respectively (b-e). Those marked with inverted triangle symbols in the bottom frame correspond to oxide contamination.

S2 Optimized Structures

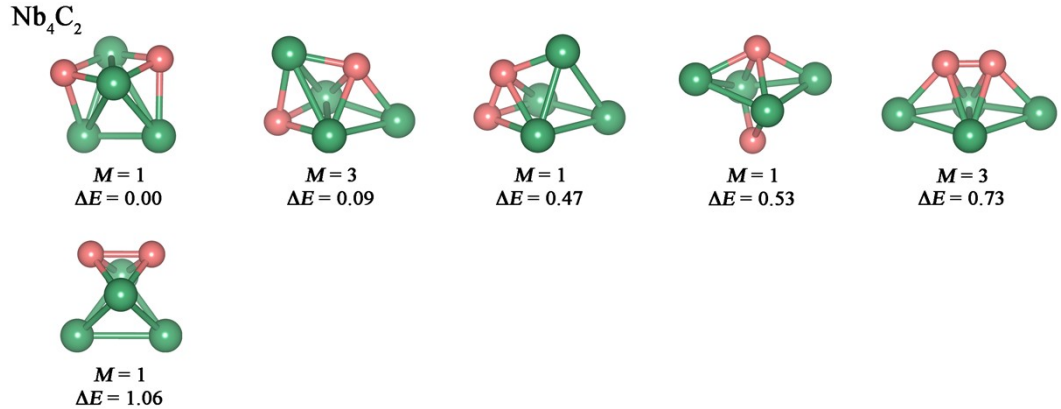


Fig. S3 Optimized structures of Nb_4C_2 . Green and pink balls represent Nb and C atoms respectively. spin multiplicities (M) and relative energies (ΔE , in units of eV, including zero-point energy, are shown below each isomer.

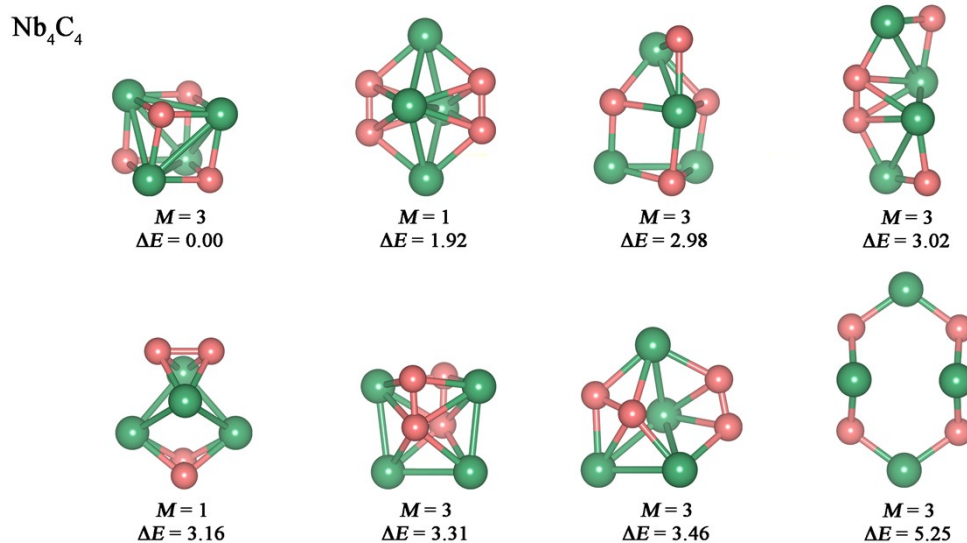


Fig. S4 Optimized structures for Nb_4C_4 . Green and pink balls represent Nb and C atoms, respectively. Spin multiplicities (M) and relative energies (ΔE , in eV, including zero-point energy (ZPE)) are shown below each isomer.

Nb_6C_8

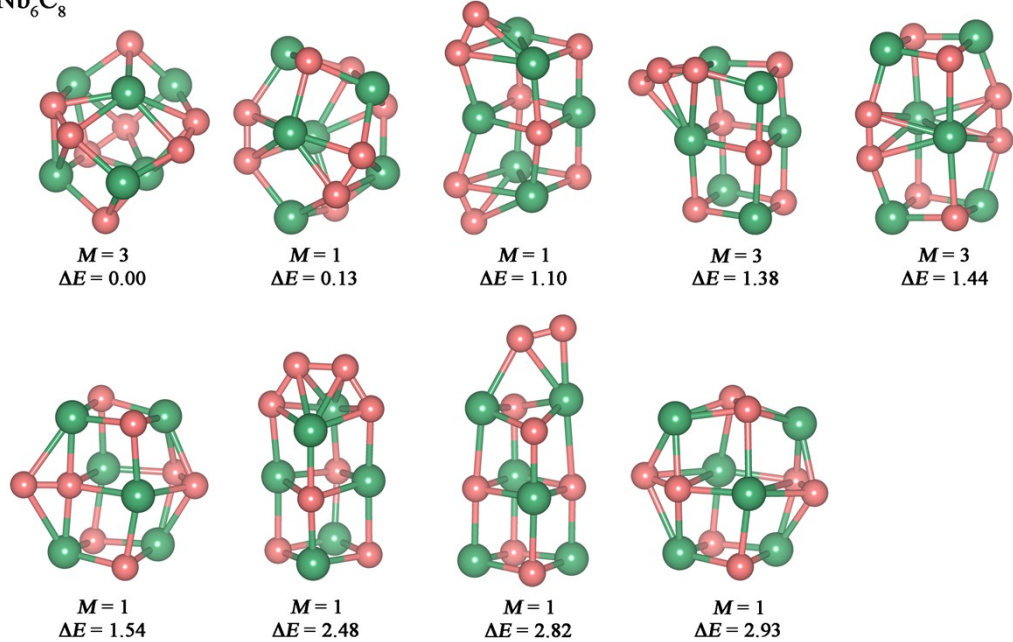


Fig. S5 Optimized structures for Nb_6C_8 . Green and pink balls represent Nb and C atoms, respectively. Spin multiplicities (M) and relative energies (ΔE , in eV, including zero-point energy (ZPE)) are shown below each isomer.

Nb_8C_{12}

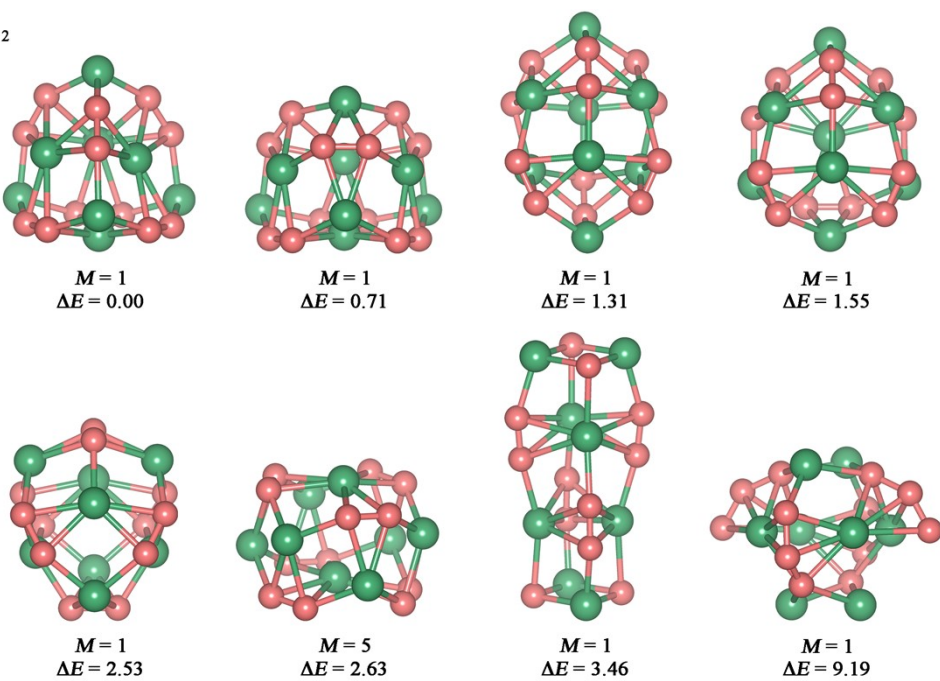


Fig. S6 Optimized structures for Nb_8C_{12} . Green and pink balls represent Nb and C atoms, respectively. Spin multiplicities (M) and relative energies (ΔE , in eV, including zero-point energy (ZPE)) are shown below each isomer.

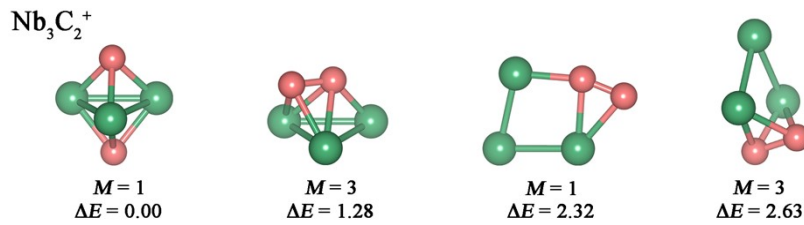


Fig. S7. Optimized structures for Nb₃C₂⁺. Green and pink balls represent Nb and C atoms, respectively. Spin multiplicities (M) and relative energies (ΔE , in eV, including zero-point energy (ZPE)) are shown below each isomer.

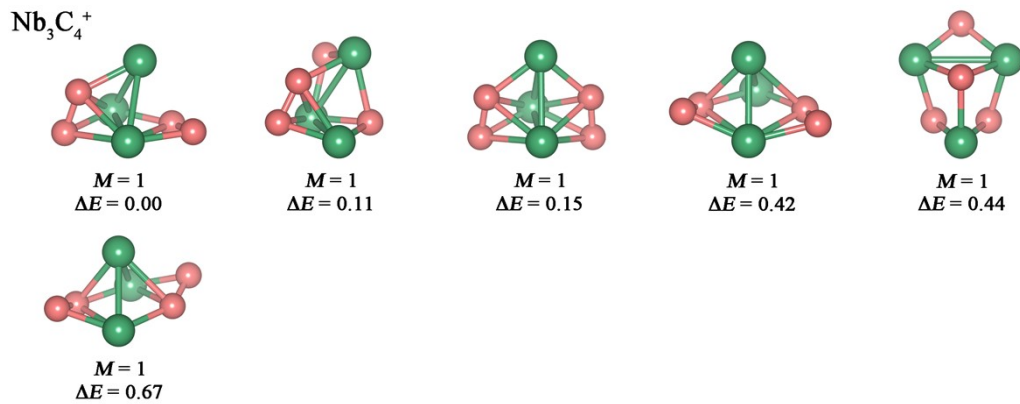


Fig. S8 Optimized structures for Nb₃C₄⁺. Green and pink balls represent Nb and C atoms, respectively. Spin multiplicities (M) and relative energies (ΔE , in eV, including zero-point energy (ZPE)) are shown below each isomer.

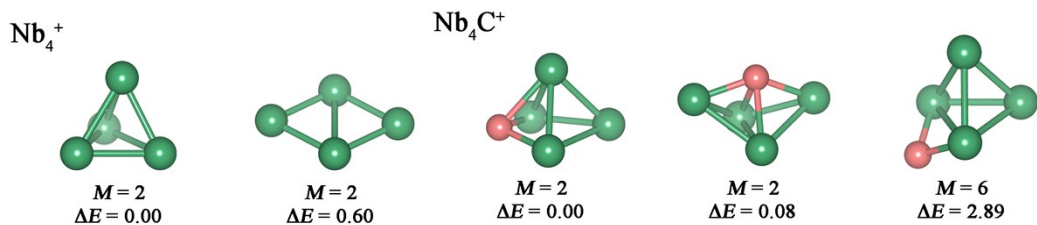


Fig. S9 Optimized structures for Nb₄⁺ and Nb₄C⁺. Green and pink balls represent Nb and C atoms, respectively. Spin multiplicities (M) and relative energies (ΔE , in eV, including zero-point energy (ZPE)) are shown below each isomer.

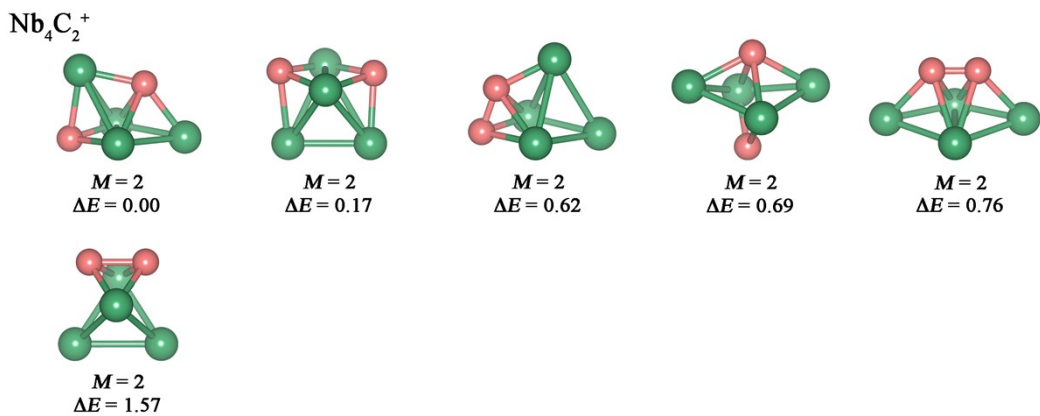


Fig. S10 Optimized structures for Nb₄C₂⁺. Green and pink balls represent Nb and C atoms, respectively. Spin multiplicities (*M*) and relative energies (Δ*E*, in eV, including zero-point energy (ZPE)) are shown below each isomer.

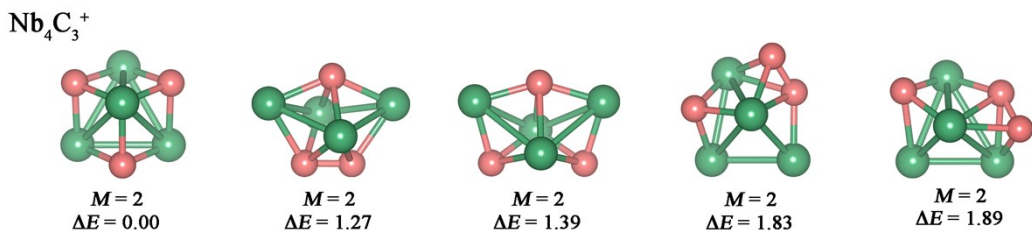


Fig. S11 Optimized structures for Nb₄C₃⁺. Green and pink balls represent Nb and C atoms, respectively. Spin multiplicities (*M*) and relative energies (Δ*E*, in eV, including zero-point energy (ZPE)) are shown below each isomer.

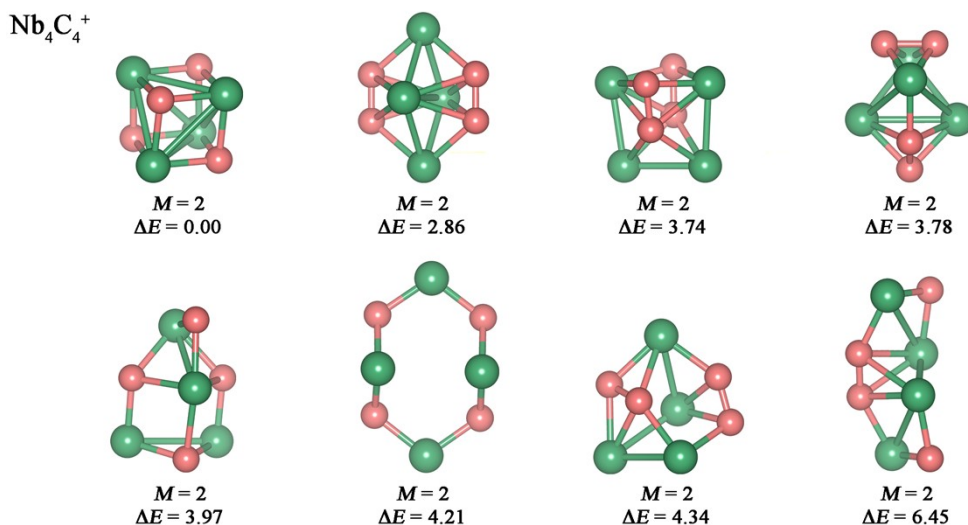


Fig. S12 Optimized structures for Nb₄C₄⁺. Green and pink balls represent Nb and C atoms, respectively. Spin multiplicities (*M*) and relative energies (Δ*E*, in eV, including zero-point energy (ZPE)) are shown below each isomer.

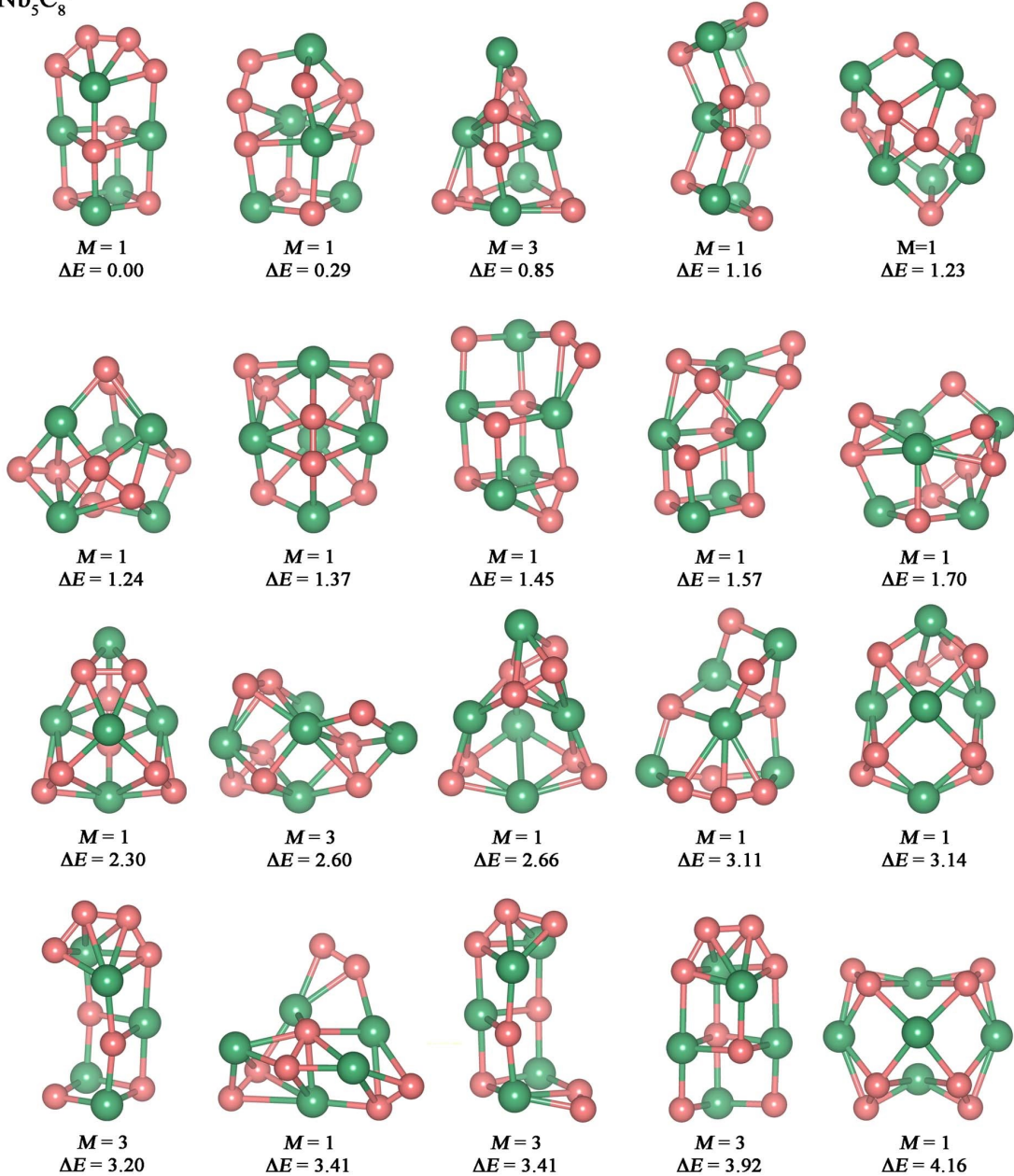
Nb_5C_8^+ 

Fig. S13 Optimized structures for Nb_5C_8^+ . Green and pink balls represent Nb and C atoms, respectively. Spin multiplicities (M) and relative energies (ΔE , in eV, including zero-point energy (ZPE)) are shown below each isomer.

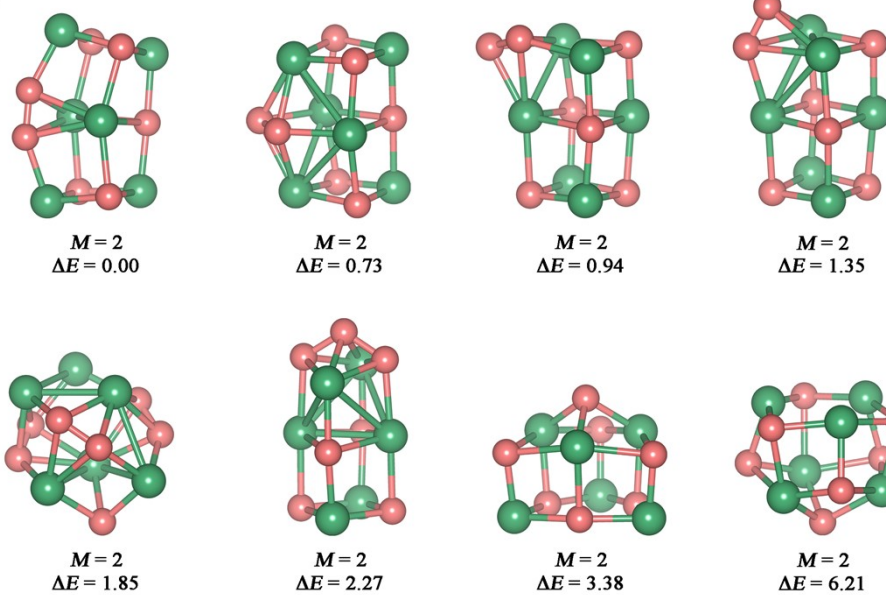
Nb_6C_7^+ 

Fig. S14 Optimized structures for Nb_6C_7^+ . Green and pink balls represent Nb and C atoms, respectively. Spin multiplicities (M) and relative energies (ΔE , in eV, including zero-point energy (ZPE)) are shown below each isomer.

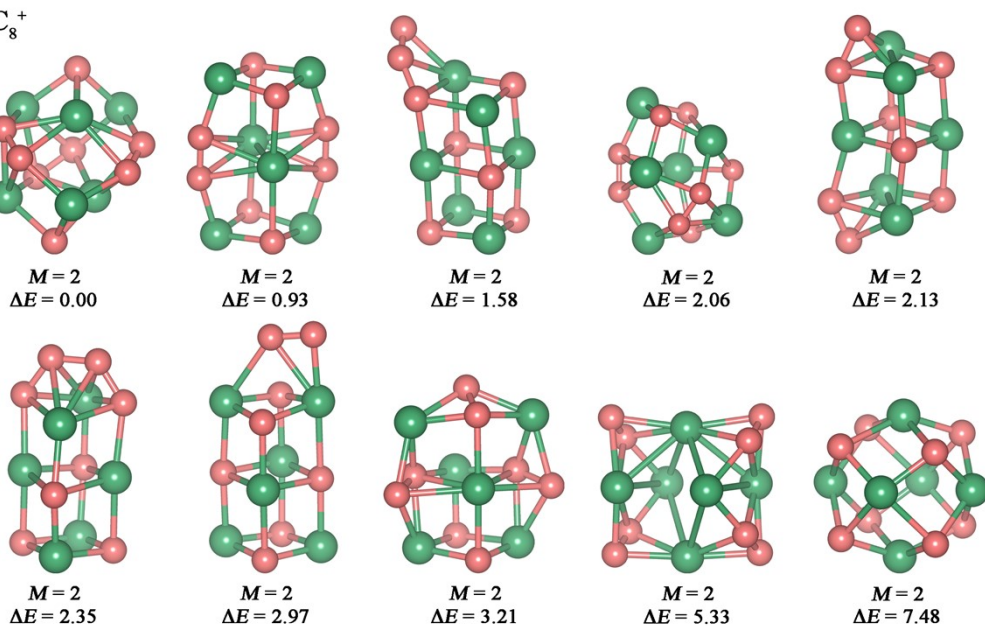
 Nb_6C_8^+ 

Fig. S15 Optimized structures for Nb_6C_8^+ . Green and pink balls represent Nb and C atoms, respectively. Spin multiplicities (M) and relative energies (ΔE , in eV, including zero-point energy (ZPE)) are shown below each isomer.

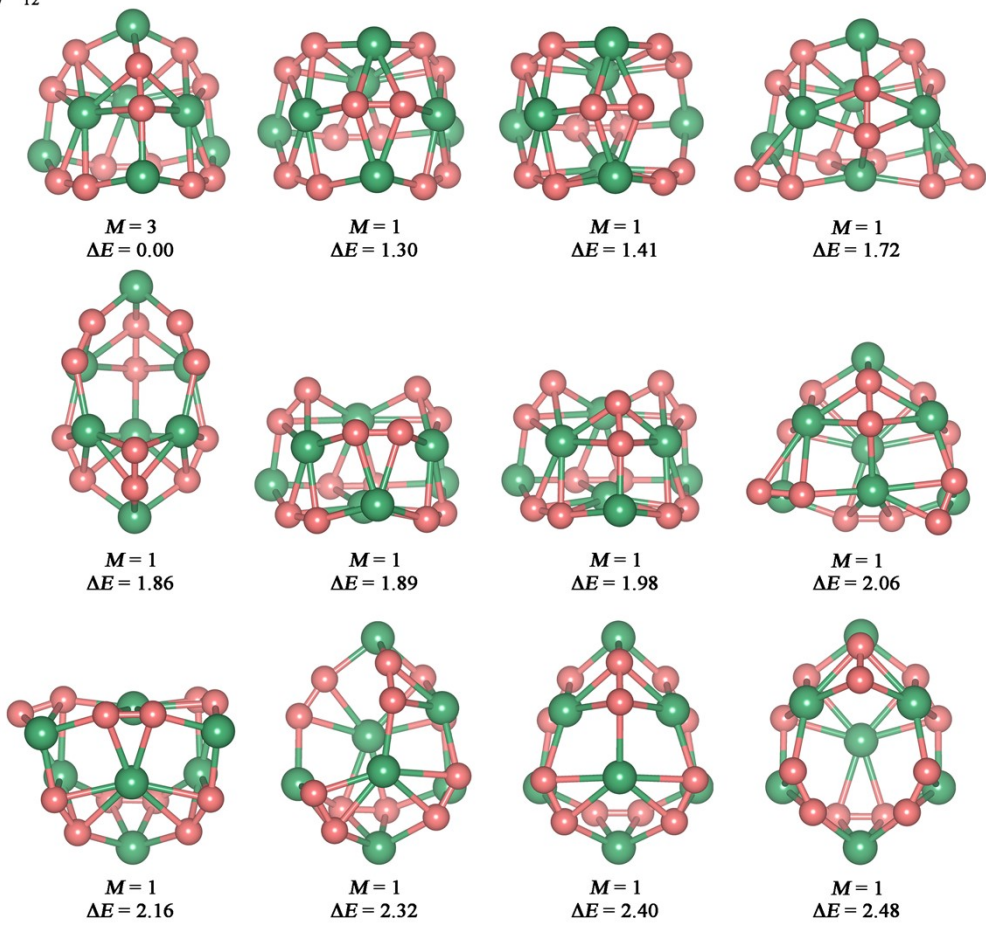
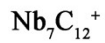


Fig. S16 Optimized structures for $\text{Nb}_7\text{C}_{12}^+$. Green and pink balls represent Nb and C atoms, respectively. Spin multiplicities (M) and relative energies (ΔE , in eV, including zero-point energy (ZPE)) are shown below each isomer.

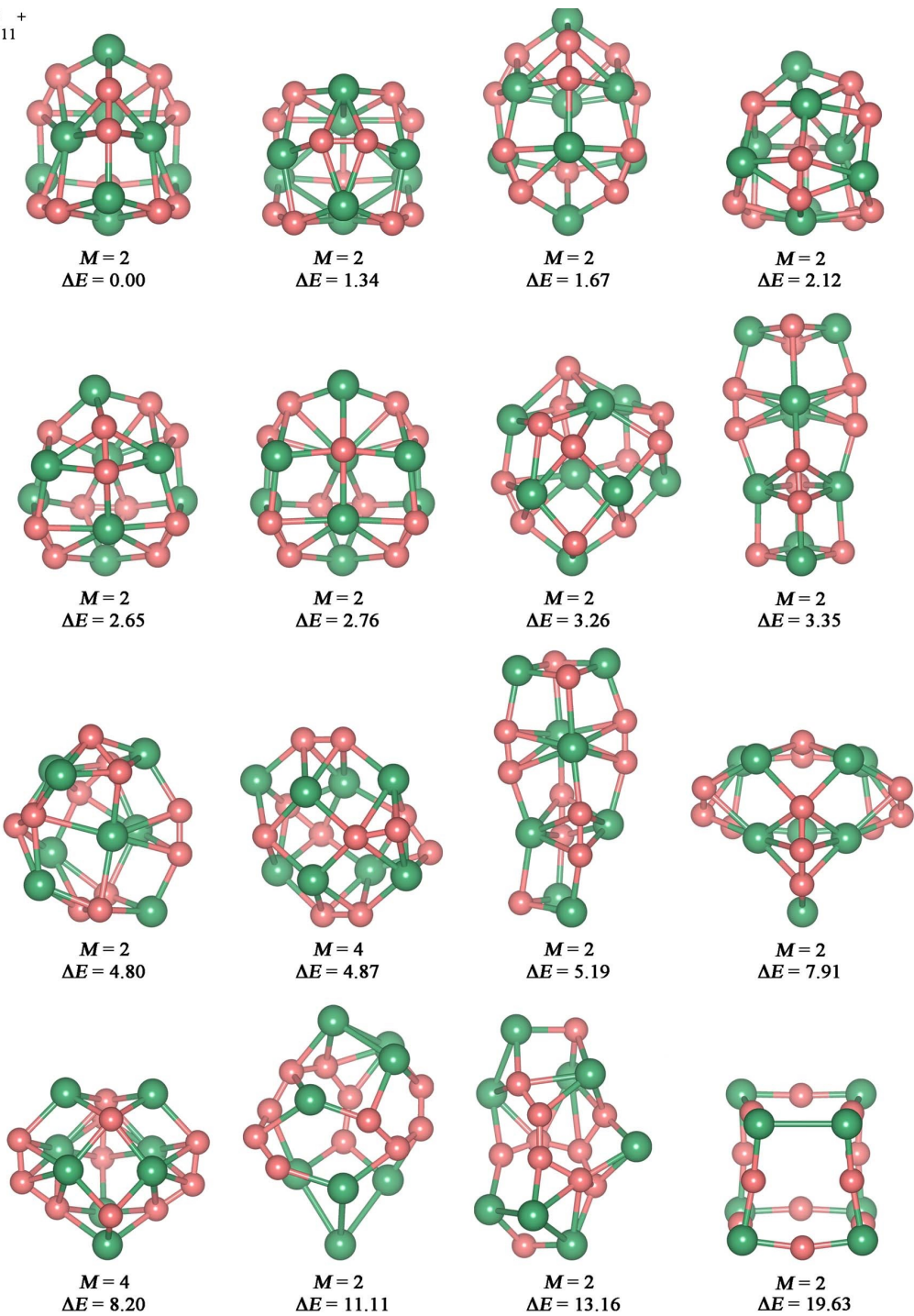
$\text{Nb}_8\text{C}_{11}^+$ 

Fig. S17 Optimized structures for $\text{Nb}_8\text{C}_{11}^+$. Green and pink balls represent Nb and C atoms, respectively. Spin multiplicities (M) and relative energies (ΔE , in eV, including zero-point energy (ZPE)) are shown below each isomer.

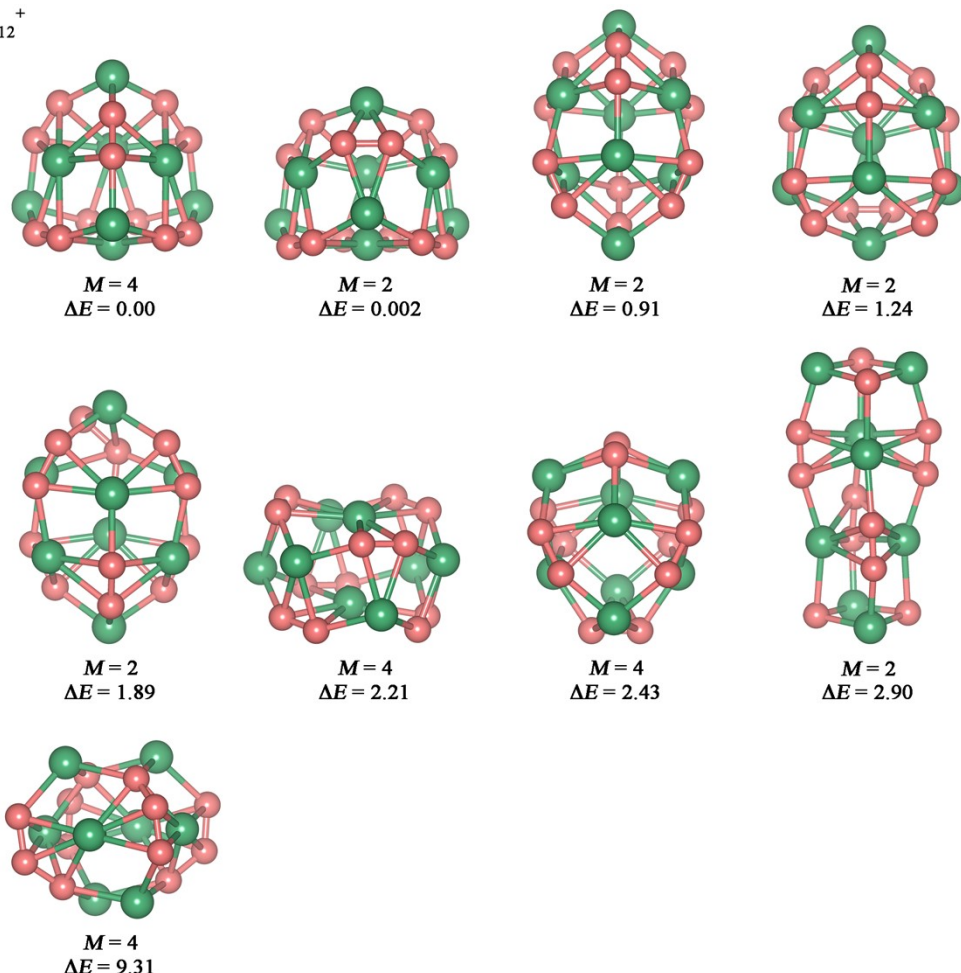


Fig. S18 Optimized structures for $\text{Nb}_8\text{C}_{12}^+$. Green and pink balls represent Nb and C atoms, respectively. Spin multiplicities (M) and relative energies (ΔE , in eV, including zero-point energy (ZPE)) are shown below each isomer.

S3 Energetics

Table S1. Calculated energetics of the Nb_nC_m^+ clusters.

	α HOMO-LUMO gap	β HOMO-LUMO gap	AEA	$E_b(\text{Nb})$	$E_b(\text{C})$
Nb_4C_2^+	0.37	1.04	5.37	5.09	7.76
Nb_4C_4^+	0.90	0.64	4.54	8.42	8.11
Nb_6C_8^+	0.26	1.14	5.27	7.14	6.20
$\text{Nb}_8\text{C}_{12}^+$	0.59	0.61	5.82	7.04	6.43

^a Energies are given in units of eV, including zero-point energy (ZPE). ^b AEA are the adiabatic electron affinity of the cluster ions. ^c $E_b(\text{Nb})$ are the binding energy of a Nb atom to Nb_nC_m^+ clusters, which is defined as $-E(\text{Nb}_n\text{C}_m^+) + E(\text{Nb}_{n-1}\text{C}_m^+) + E(\text{Nb})$, and $E_b(\text{C})$ are the binding energy of a C atom to Nb_nC_m^+ clusters, which is defined as $-E(\text{Nb}_n\text{C}_m^+) + E(\text{Nb}_{n-1}\text{C}_{m-1}^+) + E(\text{C})$.

S4 Bonding Nature of Nb_4C_4^+

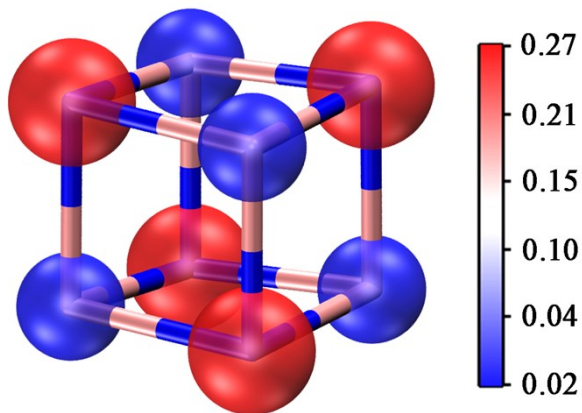


Fig. S19 DFT calculation result of the Spin population analysis for Nb_4C_4^+ .

Table S2. Bond order analysis of Nb_4C_4^+ .

	Nb1-Nb2/4	Nb1-Nb3	Nb1-C6/8	Nb1-C7	Nb1-C7	Nb2-C6	C6-C8/5	C5-C8
Mayer	0.65	0.72	1.06	1.20	-	-	-	-
Wiberg	0.66	0.72	1.32	1.48	0.099	0.12	0.13	

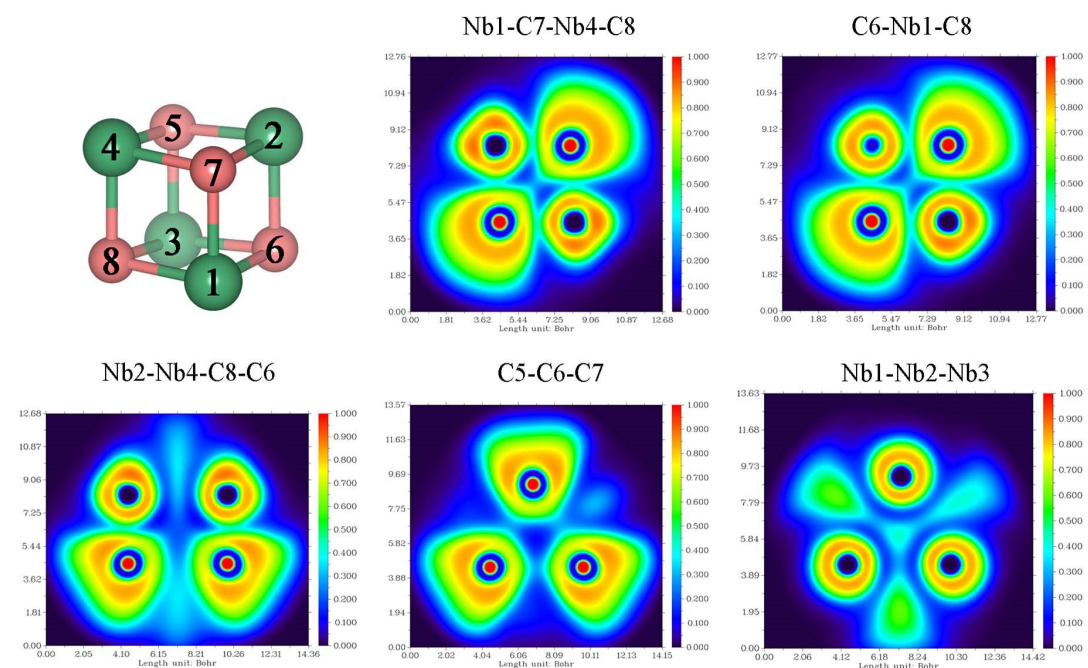


Fig. S20 Electron localization function (ELF) analysis at the different planes of Nb_4C_4^+ .

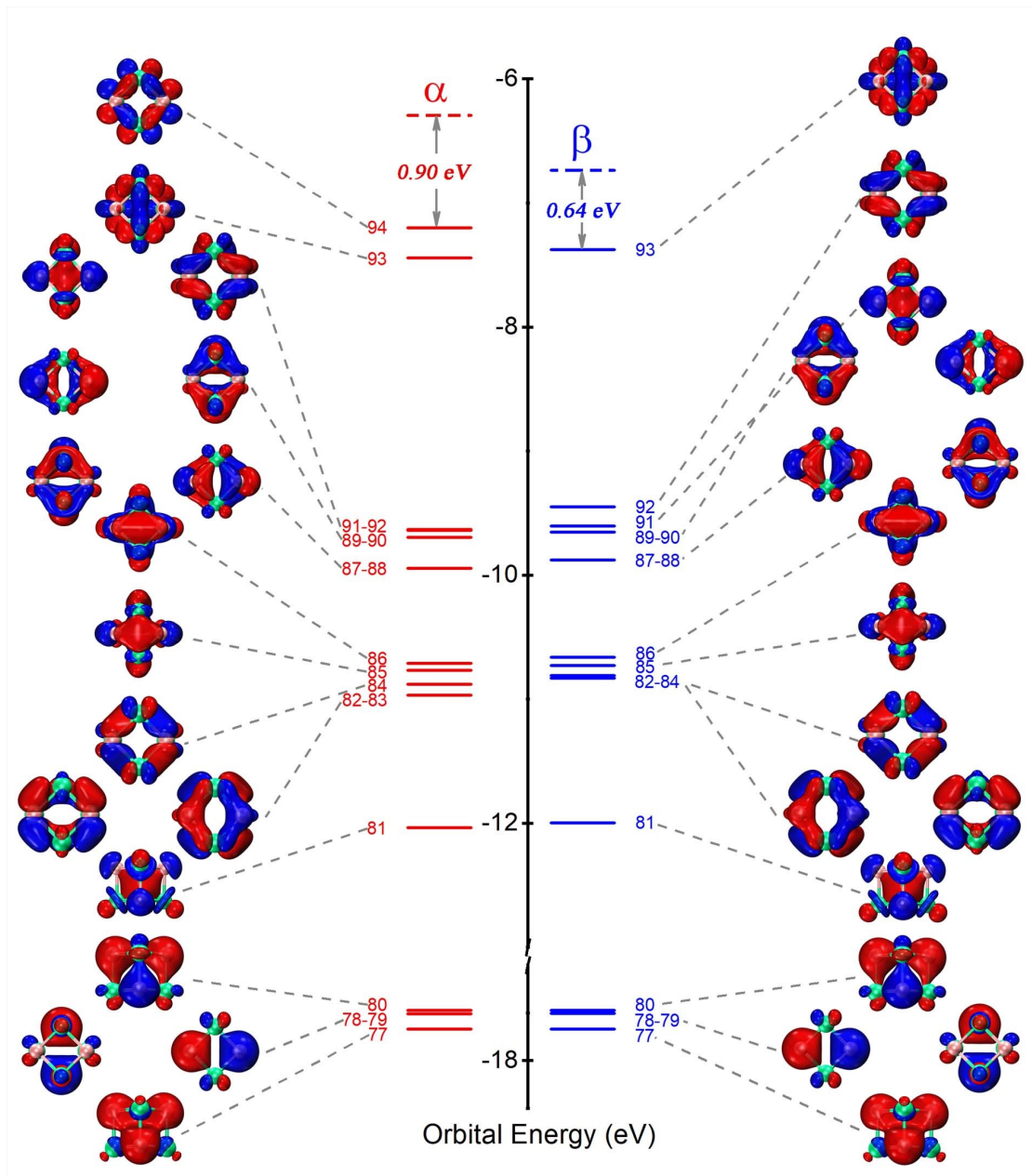


Fig. S21 DFT-calculated frontier canonical molecular orbitals of Nb_4C_4^+ .

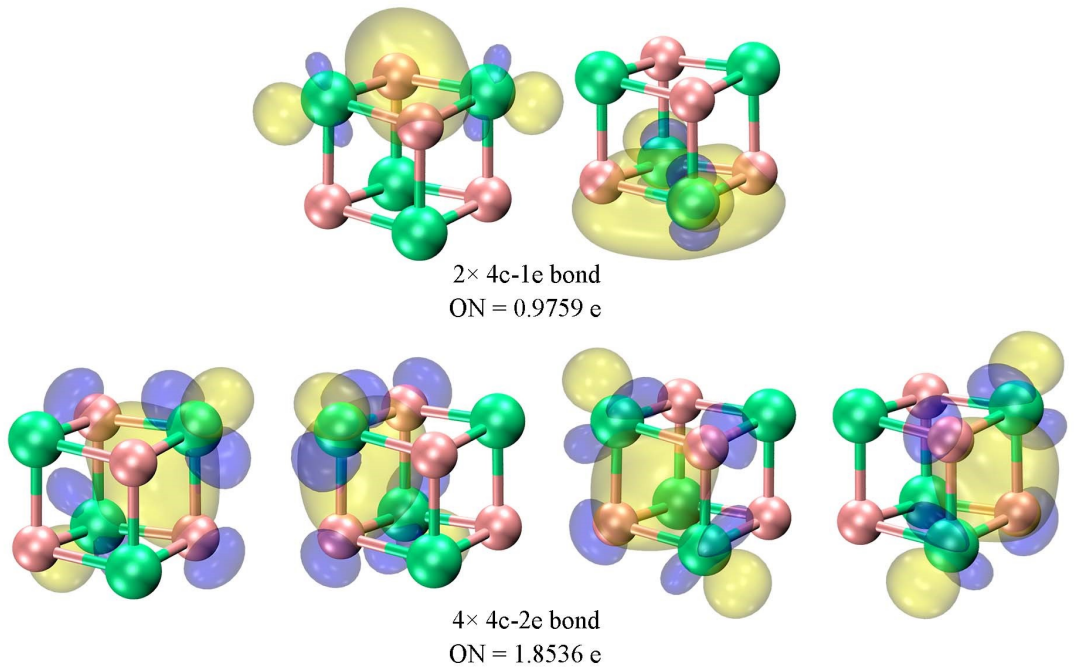


Fig. S22 AdNP bonding patterns with the occupation numbers (ON) indicated of D_{2d} Nb_4C_4^+ .

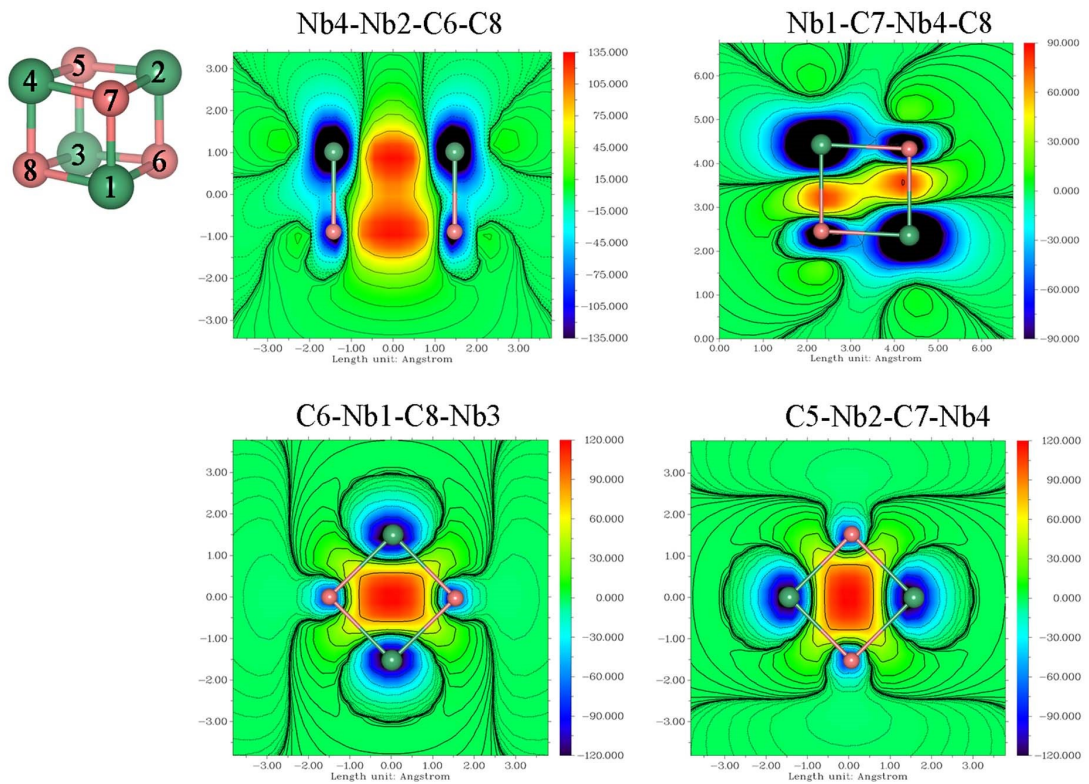


Fig. S23 The iso-chemical shielding surface (ICSSs) at the different planes of Nb_4C_4^+ .

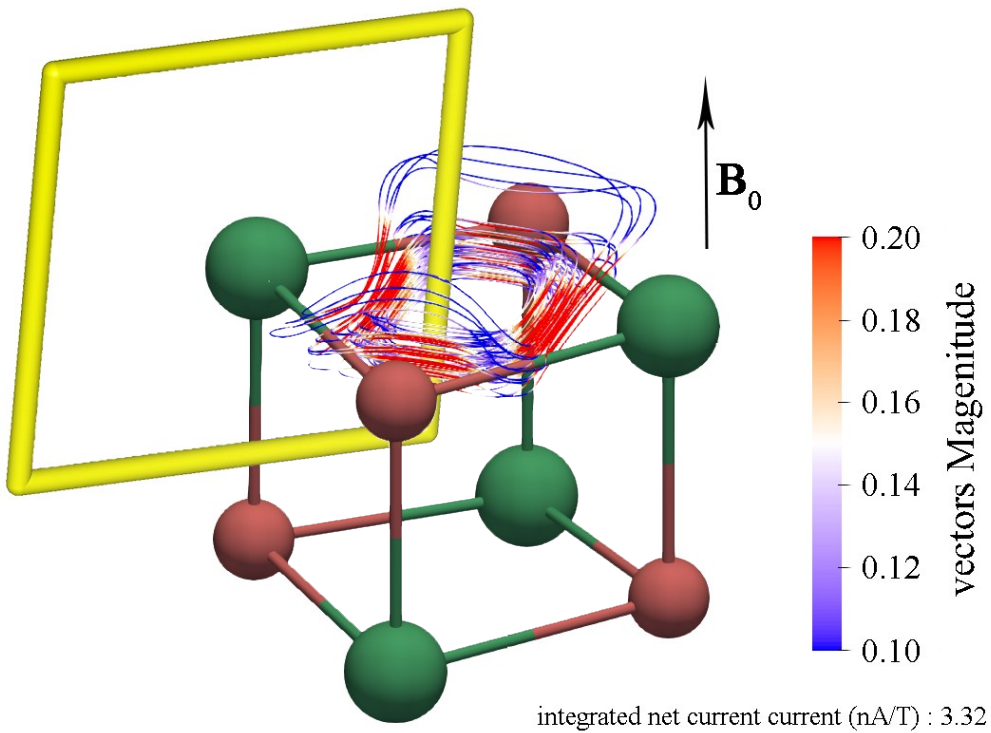


Fig. S24 The gauge including magnetically induced current (GIMIC) of Nb_4C_4^+ when the external magnetic field in the [0,0,1] direction (Z) is applied, with the integral of the induced current that crosses the defined section is labeled below.

S5 Interaction and Energy Decomposition Analysis

Table S3. DFT-Calculated average bond lengths and average Wiberg bond order of the $\text{Nb}_n(\text{C}_2\text{H}_2)_m^+$, $\text{Nb}_n(\text{C}_2\text{H}_4)_m^+$ and Nb_4C_4^+ clusters.

	Nb-Nb length	Nb-C order	Nb-C length	Nb-C order	C-C length	C-C order	C-H length	C-H order
Nb_4^+	2.55	2.00	-	-	-	-	-	-
C_2H_2	-	-	-	-	1.21	3.11	1.06	0.94
C_2H_4	-	-	-	-	1.34	2.15	1.09	0.94
$\text{Nb}_4(\text{C}_2\text{H}_2)_2^+$	2.69	1.28	2.18	0.87	1.43	1.41	1.10	0.85
$\text{Nb}_4(\text{C}_2\text{H}_4)_2^+$	2.58	1.61	2.30	0.69	1.46	1.30	1.10	0.86
Nb_4C_4^+	2.90	0.68	2.01	1.38	2.80	0.13	-	-

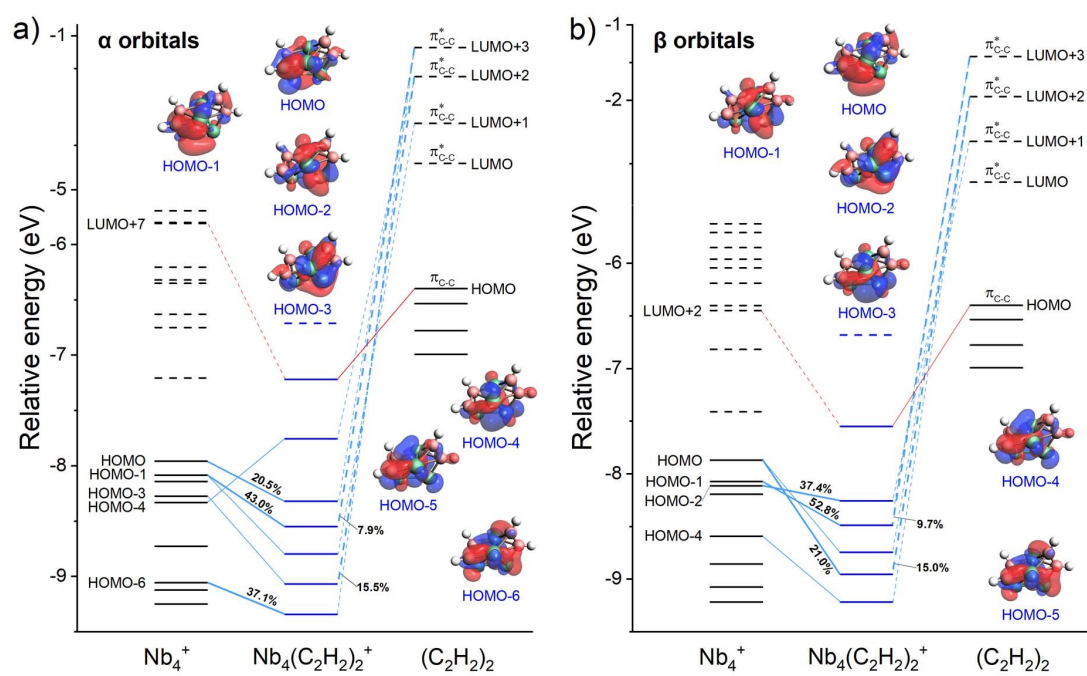


Fig. S25 Energy level correlation of α frontier orbitals (a), and β frontier orbitals (b) in $\text{Nb}_4(\text{C}_2\text{H}_2)_2^+$ cluster, and insets show the corresponding orbitals of $\text{Nb}_4(\text{C}_2\text{H}_4)_2^+$ cluster.

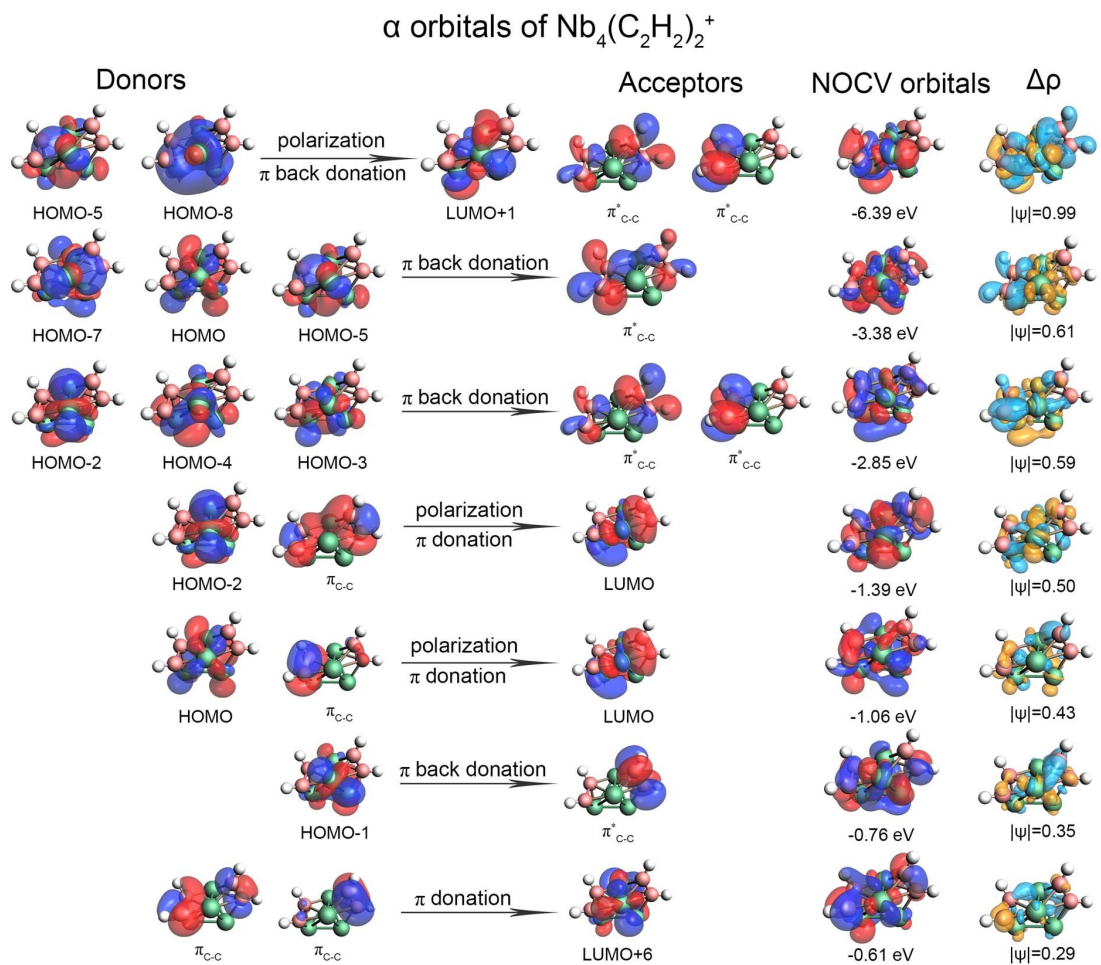


Fig. S26 Natural orbitals for chemical valence (NOCV) pair of α orbitals ψ (eigenvalues given in parenthesis), and the corresponding NOCV deformation electron density plots $\Delta\rho$ between Nb_4^+ and $(\text{C}_2\text{H}_2)_2$. The color code of the charge flow is red \rightarrow blue. The isosurface values are ± 0.03 a.u. for symmetrized fragment orbitals (SFOs) and NOCV orbitals, ± 0.00015 a.u. for $\Delta\rho$, respectively.

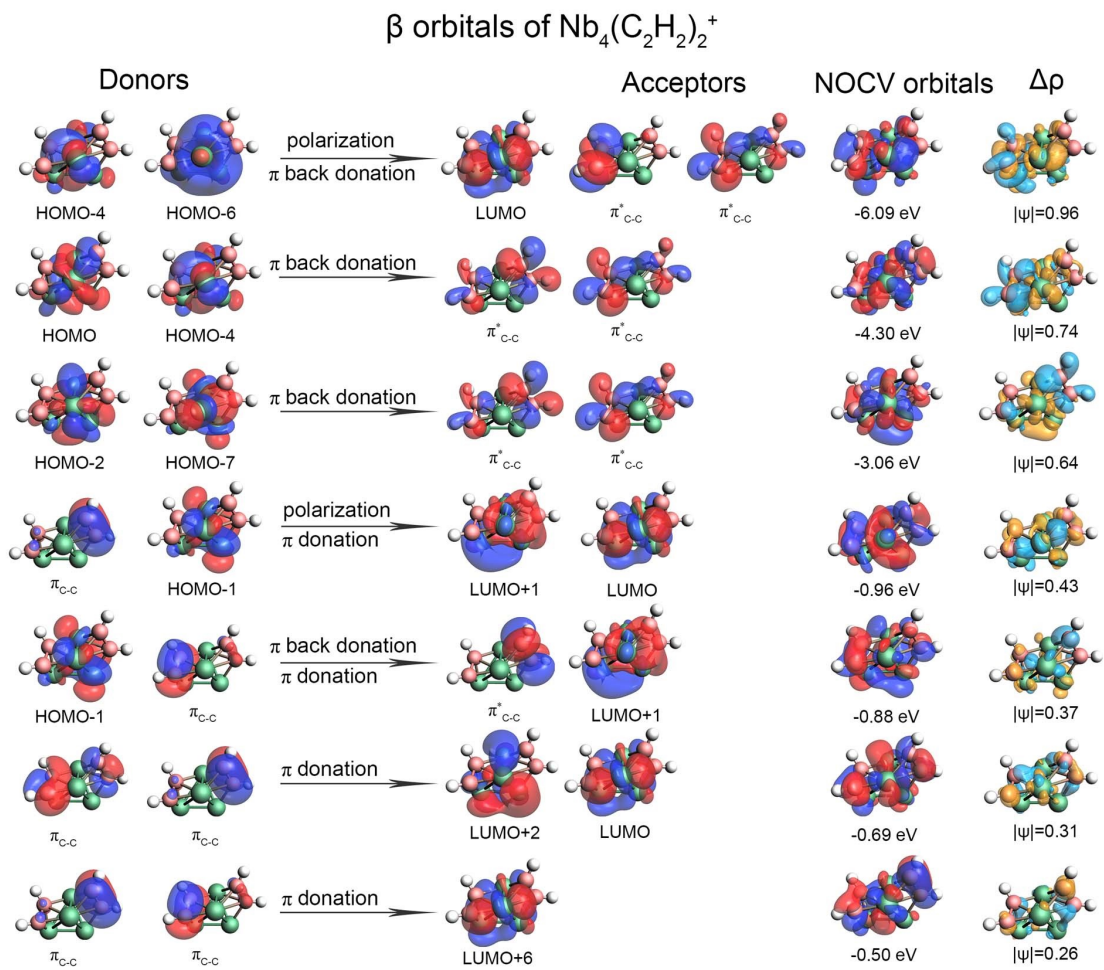


Fig. 27 Natural orbitals for chemical valence (NOCV) pair of β orbitals Ψ (eigenvalues given in parenthesis), and the corresponding NOCV deformation electron density plots $\Delta\rho$ between Nb_4^+ and $(\text{C}_2\text{H}_2)_2$. The color code of the charge flow is red \rightarrow blue. The isosurface values are ± 0.03 a.u. for symmetrized fragment orbitals (SFOs) and NOCV orbitals, ± 0.00015 a.u. for $\Delta\rho$, respectively.

Table S4. EDA results for $\text{Nb}_4(\text{C}_2\text{H}_2)_2^+$ cluster using ADF at the PW91/TZ2P-ZORA level, taking Nb_4^+ and $(\text{C}_2\text{H}_2)_2$ as interacting fragments. Total bonding energy $\Delta E_{\text{int}} = \Delta E_{\text{pauli}} + \Delta E_{\text{ele}} + \Delta E_{\text{orb}}$, where ΔE_{pauli} is the repulsion energy caused by the Pauli exclusion principle, ΔE_{ele} and ΔE_{orb} are the attraction energies due to electrostatic and orbital interactions respectively. Energies are given in eV.

$\text{Nb}_4(\text{C}_2\text{H}_2)_2^+$		
Energy term	Assignment	eV
ΔE_{int}	-	-13.46
ΔE_{pauli}	-	56.57
ΔE_{ele}	-	-34.40
ΔE_{orb}	-	-35.63
$\Delta E_{\text{orb-}\alpha(1)}$	π back donation	-6.39(17.93%)
$\Delta E_{\text{orb-}\beta(1)}$	polarization + π back donation	-6.09(17.09%)
$\Delta E_{\text{orb-}\beta(2)}$	π back donation	-4.30(12.07%)
$\Delta E_{\text{orb-}\alpha(2)}$	π back donation	-3.38(9.49%)
$\Delta E_{\text{orb-}\beta(3)}$	π back donation	-3.06(8.59%)
$\Delta E_{\text{orb-}\alpha(3)}$	π back donation	-2.85(8.00%)
$\Delta E_{\text{orb-}\alpha(4)}$	polarization+ π donation	-1.39(3.90%)
$\Delta E_{\text{orb-}\alpha(5)}$	polarization + π donation	-1.06(2.98%)
$\Delta E_{\text{orb-}\beta(4)}$	polarization+ π donation	-0.96(2.69%)
$\Delta E_{\text{orb-}\beta(5)}$	π donation + π back donation	-0.88(2.47%)
$\Delta E_{\text{orb-}\alpha(6)}$	π back donation	-0.76(2.13%)
$\Delta E_{\text{orb-}\beta(6)}$	π donation	-0.69(1.94%)
$\Delta E_{\text{orb-}\alpha(7)}$	π donation	-0.61(1.71%)
$\Delta E_{\text{orb-}\beta(7)}$	π donation	-0.50(1.40%)
$\Delta E_{\text{orb-rest}}$	-	-2.71(7.61%)

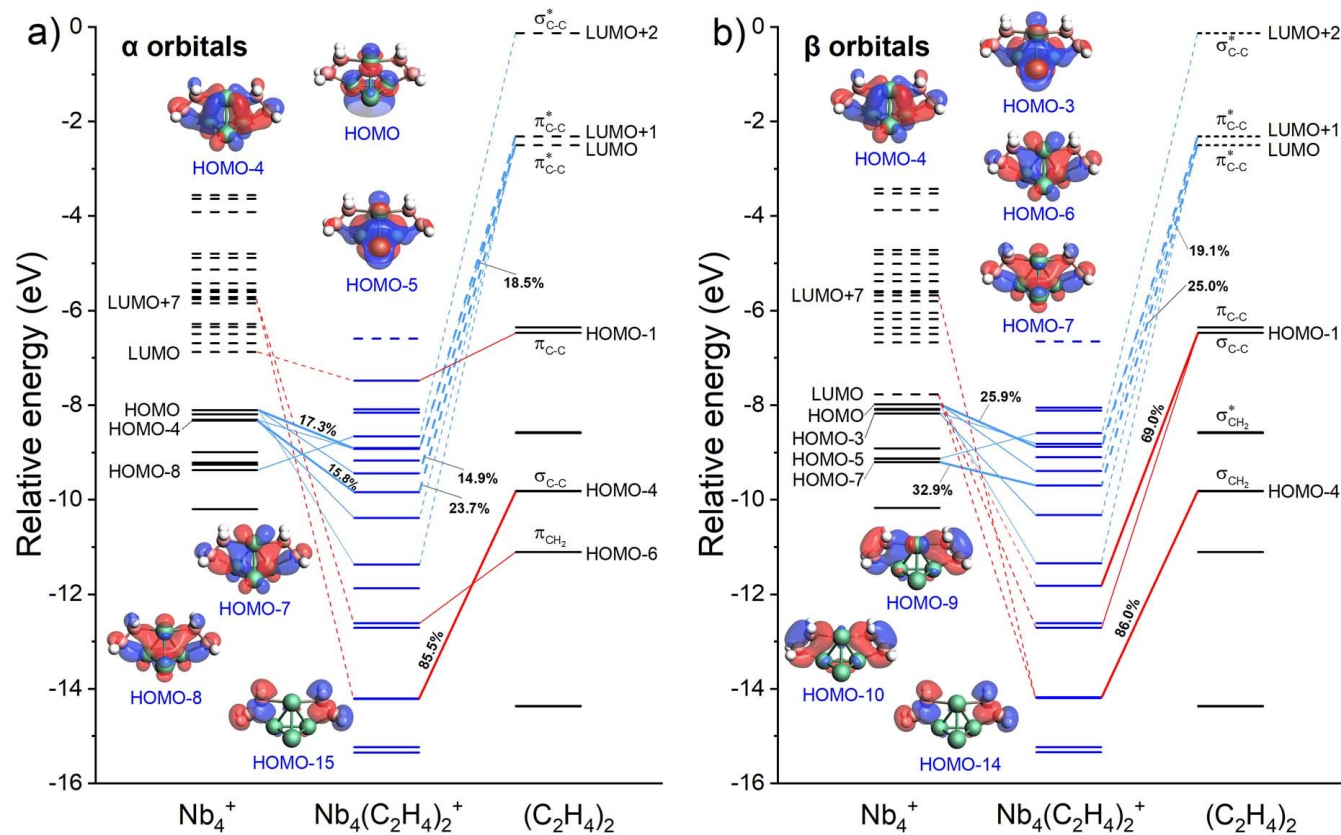


Fig. S28 Energy level correlation of α frontier orbitals (a), and β frontier orbitals (b) in $\text{Nb}_4(\text{C}_2\text{H}_4)_2^+$ cluster. Insets show the corresponding orbitals of $\text{Nb}_4(\text{C}_2\text{H}_4)_2^+$.

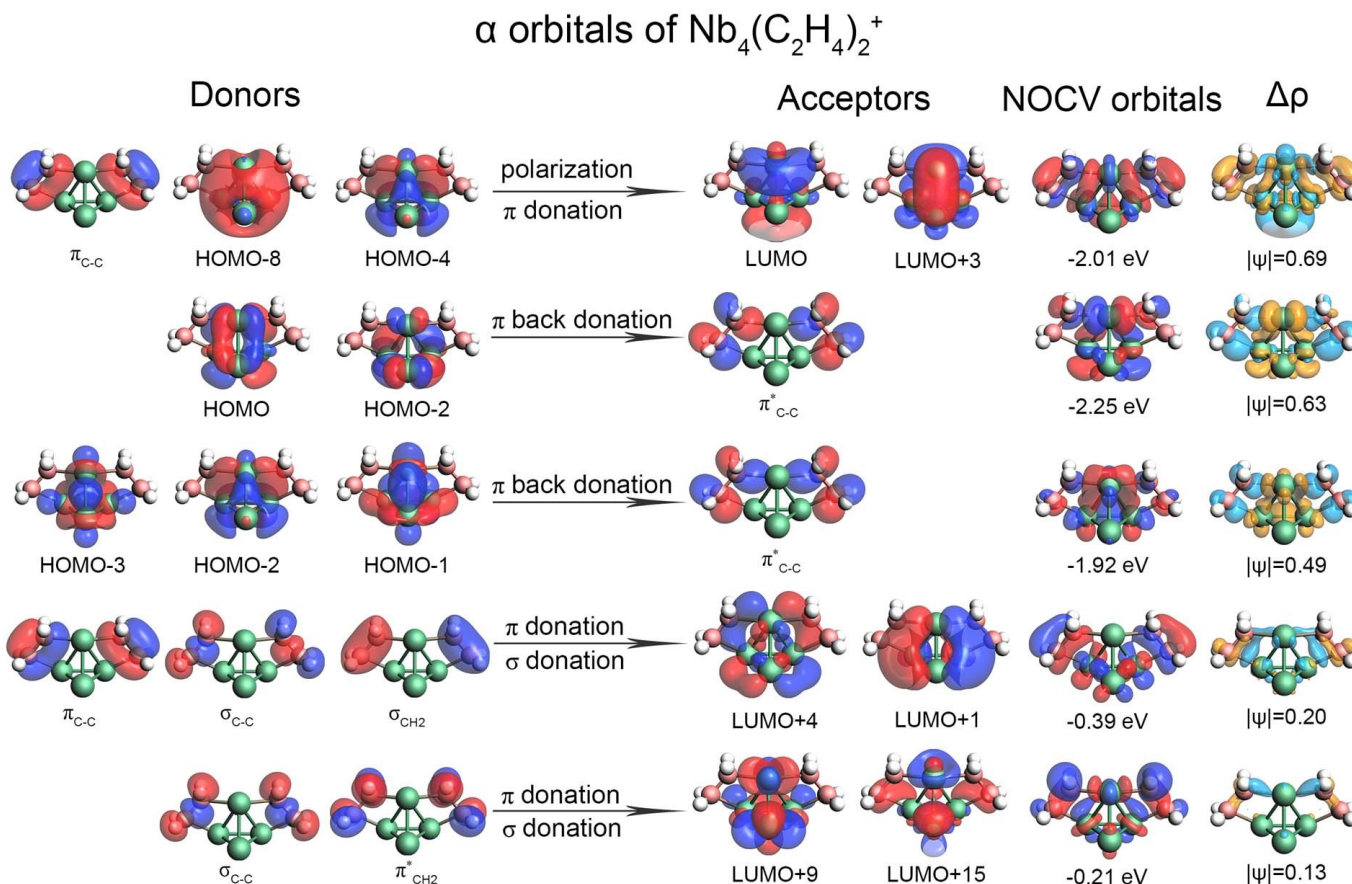


Fig. S29 Natural orbitals for chemical valence (NOCV) pair of α orbitals Ψ (eigenvalues given in parenthesis), and the corresponding NOCV deformation electron density plots $\Delta\rho$ between Nb_4^+ and $(\text{C}_2\text{H}_4)_2$. The color code of the charge flow is red \rightarrow blue. The isosurface values are ± 0.03 a.u. for symmetrized fragment orbitals (SFOs) and NOCV orbitals, ± 0.00015 a.u. for $\Delta\rho$, respectively.

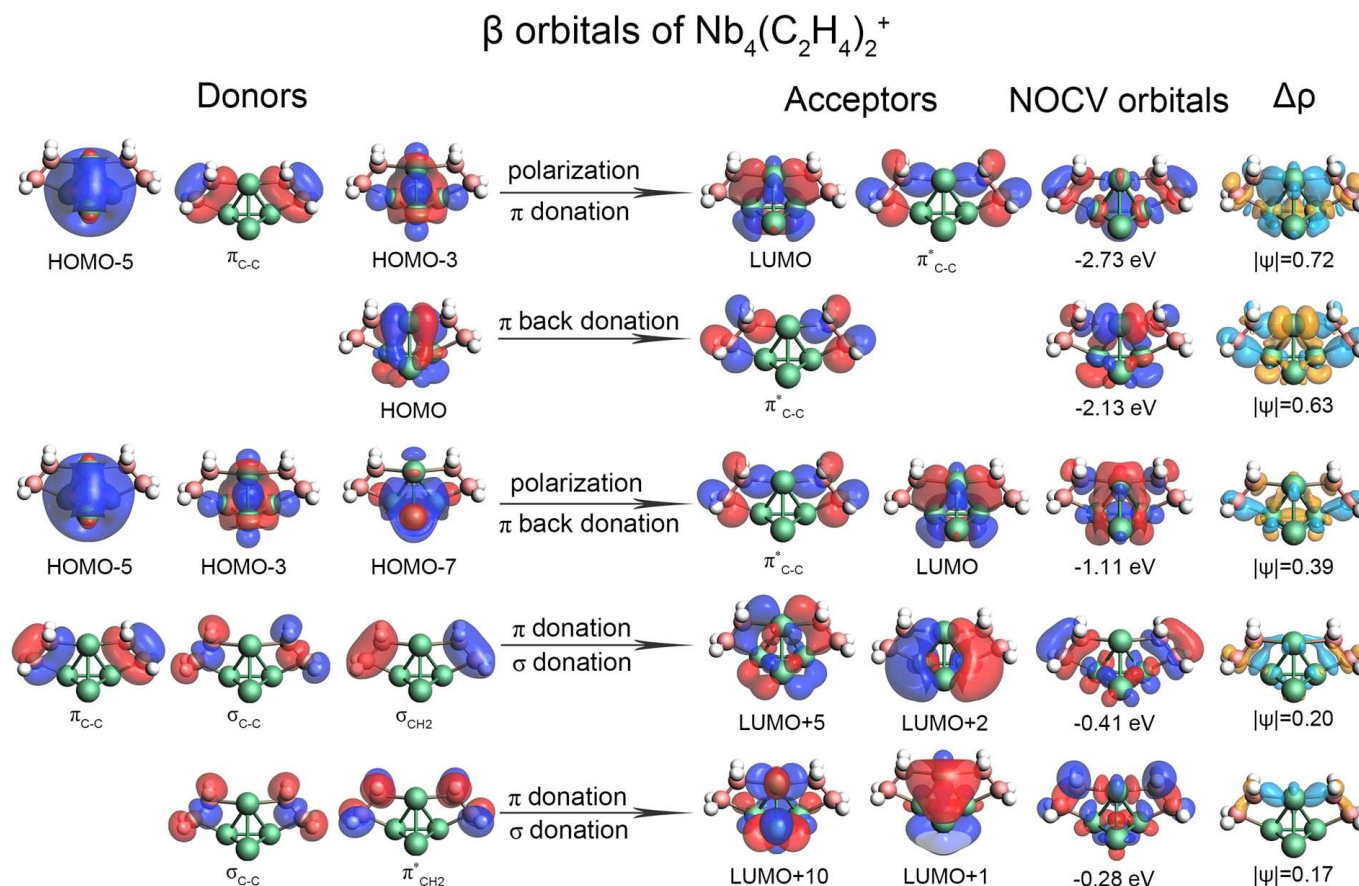


Fig. S30 Natural orbitals for chemical valence (NOCV) pair of β orbitals ψ (eigenvalues given in parenthesis), and the corresponding NOCV deformation electron density plots $\Delta\rho$ between Nb_4^+ and $(\text{C}_2\text{H}_4)_2$. The color code of the charge flow is red \rightarrow blue. The isosurface values are ± 0.03 a.u. for symmetrized fragment orbitals (SFOs) and NOCV orbitals, ± 0.00015 a.u. for $\Delta\rho$, respectively.

Table S5. EDA results for $\text{Nb}_4(\text{C}_2\text{H}_4)_2^+$ cluster using ADF at the PW91/TZ2P-ZORA level, taking Nb_4^+ and $(\text{C}_2\text{H}_4)_2$ as interacting fragments. Total bonding energy $\Delta E_{\text{int}} = \Delta E_{\text{pauli}} + \Delta E_{\text{ele}} + \Delta E_{\text{orb}}$. ΔE_{pauli} is the repulsion energy caused by the Pauli exclusion principle. ΔE_{ele} and ΔE_{orb} are the attraction energies due to electrostatic and orbital interactions, respectively. Energy values are given in eV.

Energy term	$\text{Nb}_4(\text{C}_2\text{H}_4)_2^+$ Assignment	eV
ΔE_{int}	-	-6.00
ΔE_{pauli}	-	24.31
ΔE_{ele}	-	-15.18
ΔE_{orb}	-	-15.13
$\Delta E_{\text{orb-}\beta(1)}$	polarization + π donation	-2.73(18.04%)
$\Delta E_{\text{orb-}\alpha(2)}$	π back donation	-2.25(14.87%)
$\Delta E_{\text{orb-}\beta(2)}$	π back donation	-2.13(14.08%)
$\Delta E_{\text{orb-}\alpha(1)}$	polarization+ π donation	-2.01(13.28%)
$\Delta E_{\text{orb-}\alpha(3)}$	π back donation	-1.92(12.69%)
$\Delta E_{\text{orb-}\beta(3)}$	polarization + π back donation	-1.11(7.34%)
$\Delta E_{\text{orb-}\beta(4)}$	π donation + σ donation	-0.41(2.71%)
$\Delta E_{\text{orb-}\alpha(4)}$	π donation + σ donation	-0.39(2.58%)
$\Delta E_{\text{orb-}\beta(5)}$	π donation + σ donation	-0.28(1.85%)
$\Delta E_{\text{orb-}\alpha(5)}$	π donation + σ donation	-0.21(1.39%)
$\Delta E_{\text{orb-rest}}$	-	-1.69(7.61%)

S6 Reaction Dynamics of Nb_n^+ + C_2H_2

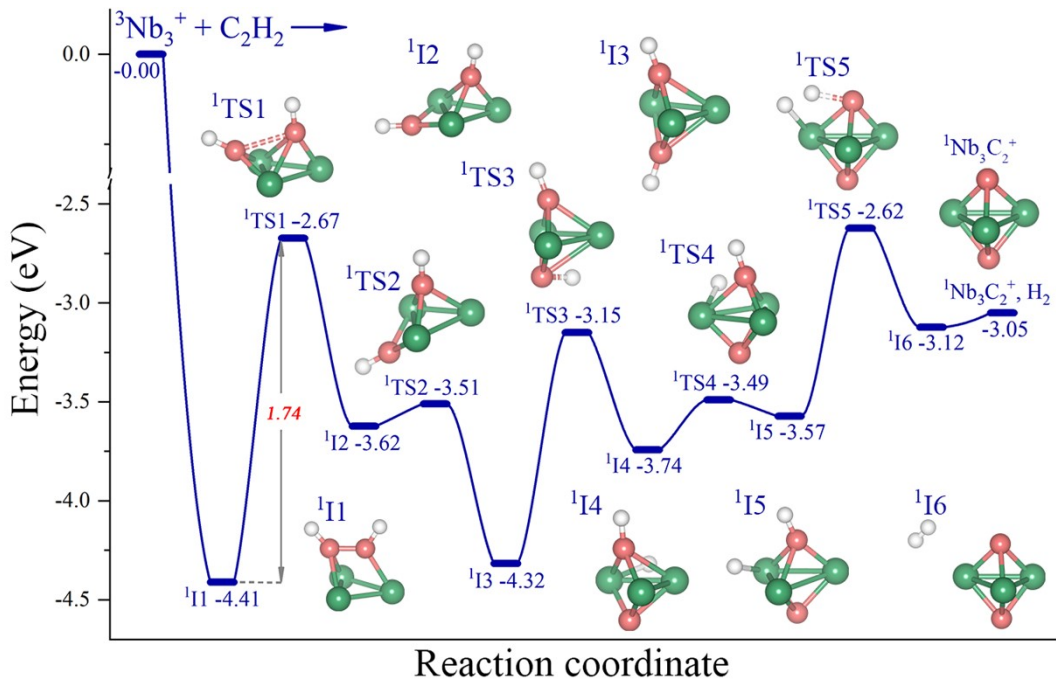


Fig. S31 The proposed reaction path for $\text{Nb}_3^+ + \text{C}_2\text{H}_2 \rightarrow \text{Nb}_3\text{C}_2^+ + \text{H}_2$.

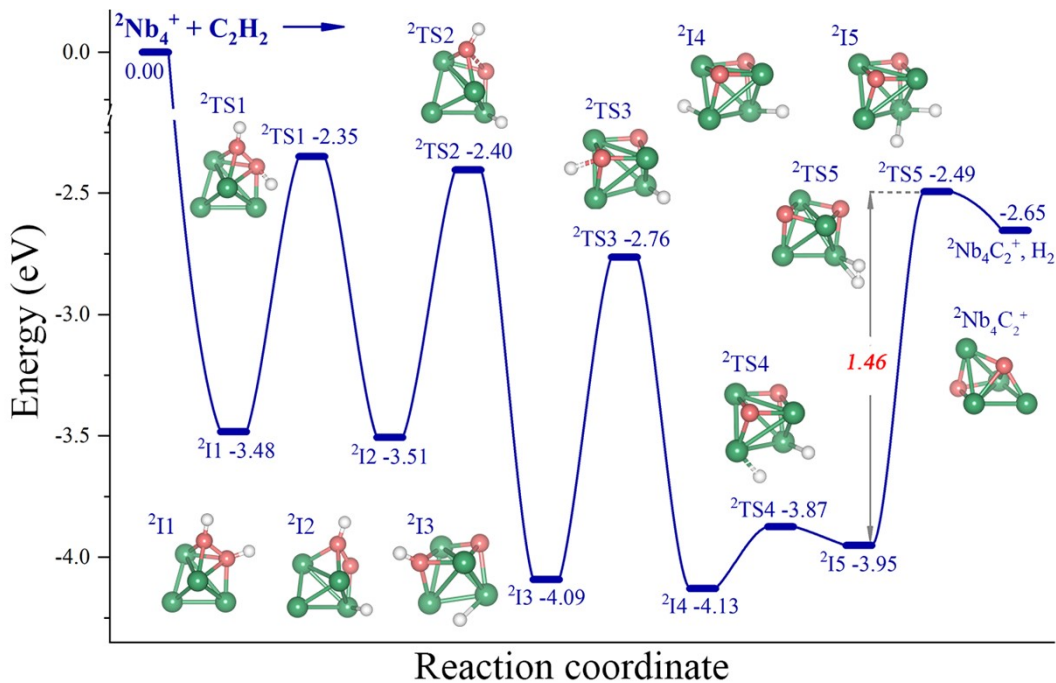


Fig. S32 The proposed reaction path1 for $\text{Nb}_4^+ + \text{C}_2\text{H}_2 \rightarrow \text{Nb}_4\text{C}_2^+ + \text{H}_2$.

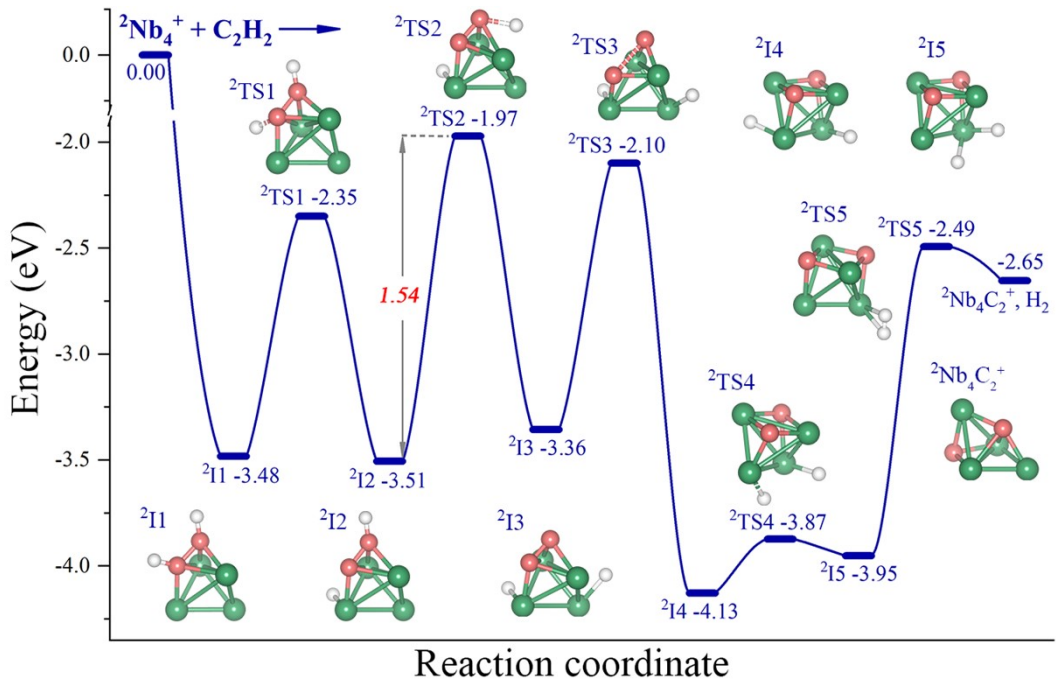


Fig. S33 The proposed reaction path2 for $\text{Nb}_4^+ + \text{C}_2\text{H}_2 \rightarrow \text{Nb}_4\text{C}_2^+ + \text{H}_2$.

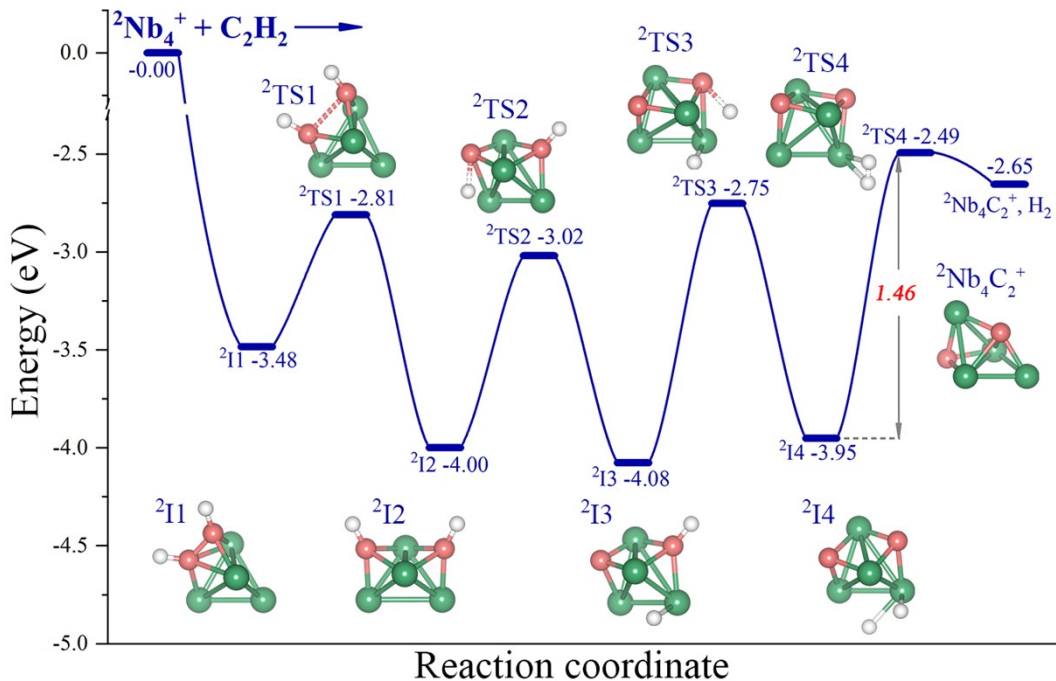


Fig. S34 The proposed reaction path3 for $\text{Nb}_4^+ + \text{C}_2\text{H}_2 \rightarrow \text{Nb}_4\text{C}_2^+ + \text{H}_2$.

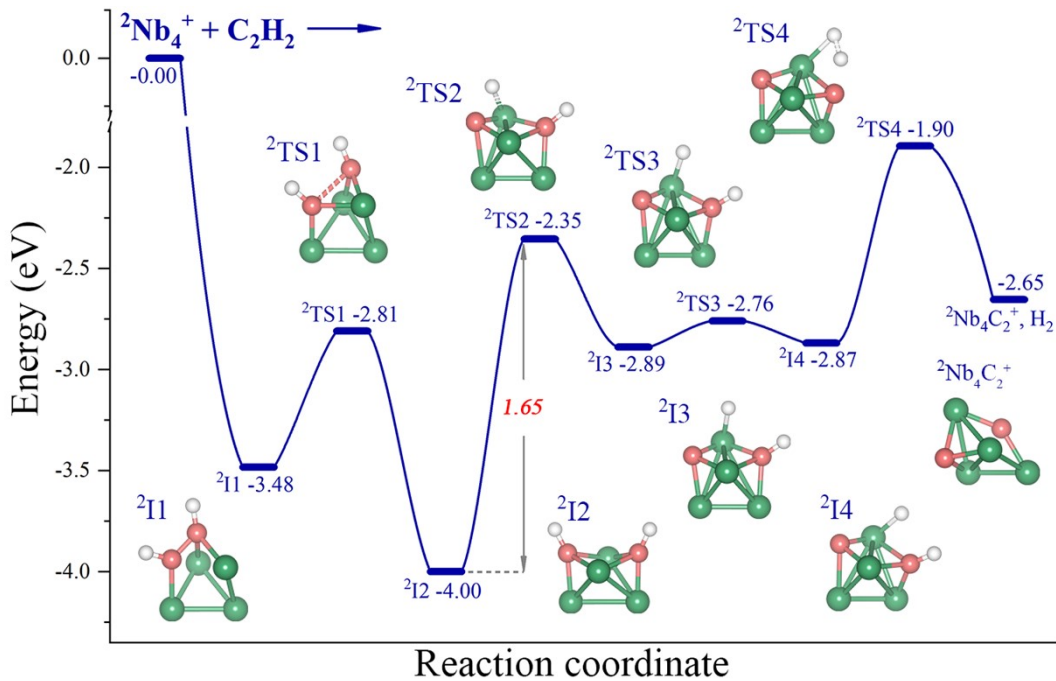


Fig. S35 The proposed reaction path4 for $\text{Nb}_4^+ + \text{C}_2\text{H}_2 \rightarrow \text{Nb}_4\text{C}_2^+ + \text{H}_2$.

Table S6. Energy comparison between different spin multiplicities ($M=2$ and $M=4$) of the structures in “ $\text{Nb}_4^+ + 2\text{C}_2\text{H}_2 \rightarrow \text{Nb}_4\text{C}_4^+ + 2\text{H}_2$ ”. The relative energies (eV) are given relative to the separated reactants (${}^2\text{Nb}_4^+ + 2\text{C}_2\text{H}_2$).

	Relative energy (eV)												
	Nb_4^+ + $2\text{C}_2\text{H}_2$	I1	I2	TS1	I3	TS2	I4	TS3	I5	TS4	I6	TS5	
$M=2$	0.00	-3.48	-5.82	-5.26	-6.77	-6.55	-6.79	-5.63	-7.08	-5.99	-7.27	-6.04	
$M=4$	0.70	-2.83	-5.54	-4.54	-6.25	-5.98	-6.00	-5.07	-6.64	-5.48	-6.12	-5.70	
	I7	TS6	I8	TS5	I7	I8	TS6	I9	TS7	I10	Nb_4C_4^+ + 2H_2		
$M=2$	-6.90	-6.08	-6.66	-6.57	-7.03	-6.92	-5.59	-6.59	-6.15	-6.73	-6.59		
$M=4$	-6.71	-5.96	-6.55	-5.82	-6.32	-6.19	-5.38	-6.42	-5.44	-6.08	-5.90		

Table S7. DFT-calculated imaginary frequencies of the transition states in “ $\text{Nb}_4^+ + 2\text{C}_2\text{H}_2 \rightarrow \text{Nb}_4\text{C}_4^+ + 2\text{H}_2$ ”.

	Frequency analysis					
Transition states	${}^2\text{TS1}$	${}^2\text{TS2}$	${}^2\text{TS3}$	${}^2\text{TS4}$	${}^2\text{TS5}$	${}^2\text{TS6}$
Imaginary frequencies (cm ⁻¹)	-342.60	-172.18	-268.34	-997.75	-675.09	-1218.21
Transition states	${}^2\text{TS5}$	${}^2\text{TS6}$	${}^2\text{TS7}$			
Imaginary frequencies (cm ⁻¹)	-1182.46	-969.11	-1012.94			